Effects of uniaxial and hydrostatic pressure on the valence band maximum in Sb_2Te_3: An electronic structure study

P. Larson
Department of Physics, Case Western Reserve University, 10900 Euclid Avenue, Cleveland, Ohio 44106, USA
(Received 5 July 2006; revised manuscript received 13 September 2006; published 15 November 2006)

Sb_2Te_3, in the form of alloys with Bi_2Te_3 and Bi_2Se_3, forms the basis of room temperature thermoelectric materials. While experimental pressure studies have investigated changes to thermoelectric properties, few theoretical investigations have examined how the band structure changes as a function of pressure. Electronic structure calculations have been performed on Sb_2Te_3 in order to understand the nature of the valence band maximum. We used lattice constants and atomic positions which have previously been relaxed under pressure in a work by another set of authors. Using these values we find significant changes to the valence band maximum as a function of pressure which the previous authors did not investigate. The valence band maximum lies off of the high symmetry lines which are usually plotted. Hydrostatic pressure shows very little change in the position of the valence band maximum up to 4 GPa, but a profound shift occurs when pressure is applied uniaxially. The valence band maximum shifts from one off-axis position to another by 2 GPa, so that around 1.5 GPa multiple valence band maxima occur which may enhance the thermoelectric properties. The effective masses of this new peak are larger, consistent with the existence of a light-hole upper valence band (UVB) and a heavy-hole lower valence band (LVB). This electronic topological transition may explain the significant increase seen in the thermoelectric properties of $Sb_{1.5}Bi_{0.5}Te_3$ as a function of uniaxial pressure around 1–2 GPa by increasing both the band degeneracy and effective masses.

DOI: 10.1103/PhysRevB.74.205113 PACS number(s): 71.20.−b, 72.20.Pa, 71.18.+y

I. INTRODUCTION

The best room temperature thermoelectric materials are based on alloys of Bi_2Te_3, Bi_2Se_3, and Sb_2Te_3. There is extensive experimental[1–6] and theoretical[7–15] work on these materials, mostly on Bi_2Te_3. The thermoelectric properties, from a band structure point of view, depend on the effective mass of the band extrema, band degeneracy, band gaps, and other intrinsic features.[16] Much theoretical and experimental work has tried to improve its already good thermoelectric qualities. This includes such changes as doping[2,5] and external pressure,[3,4,6,13,15] though hydrostatic and uniaxial pressure produce different behaviors. In $Sb_{1.5}Bi_{0.5}Te_3$ a significant increase in the thermoelectric properties is observed ~2.0 GPa uniaxial pressure[6] while in Bi_2Te_3 a sharp increase is seen for hydrostatic pressure around 2.0 GPa.[17] So far there is no complete explanation of how pressure changes the band structure in order to enhance the thermoelectric properties.

In order to understand the importance of the position of the valence band maximum with respect to the thermoelectric properties, a review of the equations describing the thermoelectric response is necessary. The maximum efficiency (or coefficient of performance) of a power generation (cooling) unit produced from thermoelectric materials depends on the dimensionless figure of merit ZT

$$ZT = \sigma S^2 T/(\kappa_L + \kappa_e), \tag{1}$$

where S is the thermopower, σ is the electrical conductivity, κ_e is the electronic thermal conductivity, and κ_L is the lattice thermal conductivity.[12] Mahan,[18] along with Hicks and Dresselhaus,[19] showed that for the anisotropic three-dimensional single-band case in the relaxation-time limit with thermal and electrical currents traveling in the same direction (x), ZT increases monotonically with the parameter B defined as

$$B = \gamma \frac{1}{3\pi^2}\left(\frac{2k_B T}{\hbar^2}\right)^{3/2}(m_x m_y m_z)^{1/2}\frac{k_B^2 T \mu_x}{e\kappa_L}, \tag{2}$$

where γ is the band degeneracy, m_i is the effective mass of the carriers (electrons or holes) in the i direction, and μ_x is the carrier mobility along the direction of transport.[10,12,20] (The B parameter was introduced by Chasmar and Stratton[21] though it has only been applied to multiple bands recently.)[10,20] The original paper by Hicks and Dresselhaus[19] mistakenly claimed that a singly degenerate band would have a larger B value than for a multiply degenerate band. The larger degeneracy factor allows for smaller fillings of individual extrema with the same carrier concentration which increases S.[9] A more complete explanation of the derivation of the thermoelectric coefficients can be found in Schiedemantel *et al.*[22]

Much is known experimentally about Sb_2Te_3 and related compounds under pressure. Under hydrostatic pressure, Sb_2Te_3 undergoes a structural transition around 8 GPa accompanied by a semiconductor to metal transition to a more hexagonal structure due to the closing of the van der Waals gap.[4,23] Thermopower values appeared fairly flat up to about 2 GPa at which point it decreases before changing sign around the transition pressure ~7–8 GPa.[3] The results differ under uniaxial pressure. A recent study focusing on the lower pressure range[6] found that in $Sb_{1.5}Bi_{0.5}Te_3$ uniaxially applied pressure at about 1.7 GPa the thermopower S increases from 212 to 305 μV/K before dropping off at higher pressures. A weak hysteresis when reversing from high pressure finds the increase in S closer to 1 GPa. Coupled with an increase in the electrical conductivity, the previous authors[6] have sug-

gested a ZT larger than 2 is possible if the thermal conductivity κ remains unchanged. This seems unlikely since, as pointed out by Thonhauser *et al.*,[15] the electrical conductivity is coupled to the thermal conductivity by the Wiedemann-Franz law. This transition is reversible but forms a complicated phase diagram with several metastable phases[3] which may be due to the greater chance of forming antisite defects under pressure.[15]

The changes in the thermoelectric properties under pressure have their root in changes to the valence band maximum. While Shubnikov–de Haas measurements have been performed,[2] precise values of the effective mass parameters are not yet known. These Shubnikov–de Haas experiments have shown the existence of two valence bands near the maximum: an upper valence band (UVB) with lighter holes and a lower valence band (LVB) with heavier holes.[2] Earlier work had the positions of these two bands reversed.[5] The separation of UVB and LVB varies with doping.[2] Neither theoretical or experimental work on Sb_2Te_3 is at the level of that on Bi_2Te_3.

A recent paper by Thonhauser *et al.*[15] studied the formation of defects, especially Sb_{Te} antisite defects, which become more likely at higher pressures. However, this could not explain the differences in the hydrostatic and uniaxial pressure data. Another recent work by Thonhauser *et al.*[13] calculated the effects of hydrostatic and uniaxial pressure on the electronic structure of Sb_2Te_3 and used these results in transport equations to predict the changes in the thermoelectric quantities such as electrical conductivity, Seebeck coefficient, and power factor. They found that hydrostatic pressure had minimal effect on the thermoelectric properties, but uniaxial pressure increased the power factor significantly. However, this paper did not investigate the positions of the band extrema. Another recent paper by Youn and Freeman[10] showed that the valence band maximum and conduction band minimum in Bi_2Te_3 do not lie along the symmetry lines shown on most band structure plots but lies off axis at a general sixfold degenerate point on the U-Γ-Z plane. Schiedemantel *et al.*[22] plotted the bands along symmetry and nonsymmetry lines to show the true valence and conduction band extrema do not lie along the symmetry lines which are usually plottted. The position of the band extrema were similar for Bi_2Te_3 in these two calculations, but not identical. Since the thermoelectric properties depend on such properties as the number carriers and their effective masses, knowing the exact position of these band extrema is extremely important.

This work will carefully investigate the changes to the positions of the band extrema in Sb_2Te_3 under pressure, specifically the valence band maximum, which can explain some of the increase in the power factor in Sb_2Te_3 under pressure. Since Sb_2Te_3 has only found to be p type[2,5] so far, we will focus on the position of the valence band maximum. The conduction band minimum does not contribute to the thermoelectric properties, plus electronic structure calculations have shown that the position of the conduction band minimum is much more difficult to determine. Disagreement has occurred between different calculations[8–11] as to the position of this band extrema. It has been shown that the $p_{1/2}$ corrections (which determine how the p orbitals are expanded when spin orbit is included) in Bi_2Te_3 shift the conduction band minimum from along Γ-Z to along Γ-a.[11] While this was also seen in Bi_2Se_3, the $p_{1/2}$ corrections in Sb_2Te_3 are negligible[11] so will not be included here.

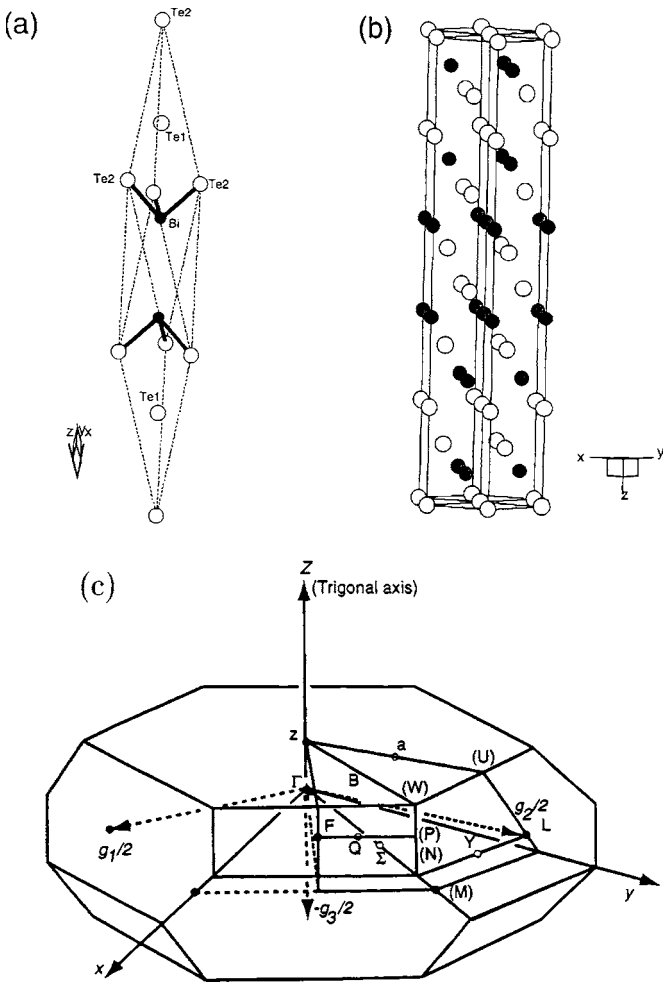

FIG. 1. (a) Crystal structure of Bi_2Te_3 (and related compounds). The five-atom "quantuple layer leaves" are separated by a van der Waals gap. Also shown are the (b) hexagonal supercell with 15 atoms and the (c) Brillouin zone.

II. CRYSTAL STRUCTURE AND METHOD

Sb_2Te_3 (as with Bi_2Te_3) forms in the tetradymite structure with the smallest unit cell having three inequivalent atoms in the rhombohedral ($R-3m$, No. 166) structure, Sb($2c$), Te_1($2c$), and Te_2($1a$). The crystal structure consists of alternating layers of Sb and Te in the order Te_1-Sb-Te_2-Sb-Te_1 to form "quintuple layer leaves" with each atom in a roughly octahedral coordination with its neighbors (Fig. 1). Strong covalent bonding is seen within and between the layers, except for Te_1 which lies along a van der Waals gap across from another Te_1 atom. The positions of the atoms in this D_{3d}^5 symmetry is that all atoms lie along the trigonal axis. Te_2 ($1a$) lies at the origin while the Sb($2c$) atoms lie at $\pm u$ ($0<u<1$) and the Te_1 ($2c$) atoms lie at $\pm v$ ($0<v<1$).[24] The relaxed lattice constants and values of u and v at differ-

TABLE I. The atomic positions (rhombohedral coordinates) of Sb and Te in Sb_2Te_3 under both hydrostatic and uniaxial pressure as calculated by Thonhauser *et al.* (Ref. 13). Experimental values are a=8.0578 a.u., b=57.5573 a.u., Sb position (u)=0.3988, and Te position (v)=0.7869 (Ref. 24).

Pressure (GPa)		0.0	1.0	2.0	3.0	4.0
Hydrostatic	a	8.2199	8.1644	8.1123	8.0630	8.0162
	c	58.287	57.893	57.524	57.174	56.842
	Sb	0.3977	0.3892	0.3987	0.3990	0.3993
	Te	0.7864	0.7876	0.7887	0.7895	0.7903
Uniaxial	a	8.2199	8.2885	8.3620	8.4412	8.5265
	c	58.287	56.981	55.649	54.286	52.887
	Sb	0.3977	0.3985	0.3987	0.3994	0.3998
	Te	0.7864	0.7879	0.7886	0.7897	0.7908

ent hydrostatic and uniaxial pressures in Sb_2Te_3 have been calculated previously by Thonhauser *et al.*,[13] so we used these values in our calculations (Table I).

Electronic structure calculations were carried out within the local spin density approximation (LSDA) to density functional theory (DFT)[25] using a full potential linear muffin tin orbital (FP-LMTO) program[26] with the exchange-correlation parametrization of Barth and Hedin.[27] This method uses an optimized basis set consisting of muffin-tin orbitals with smoothed Hankel functions as envelope functions. The smoothing radii and κ values (Hankel function decay parameters) were carefully adjusted to optimize an efficient basis set with one s, p, and d state on each Sb and Te site. The smooth interstitial quantities are calculated using a fine Fourier transform mesh and the Brillouin zone integrations were carried out with a well-converged k-mesh based on a $10\times10\times60$ division of reciprocal space. Spin-orbit interactions (SOIs) were added self-consistently in a second-variational method for all calculated band structures shown here.

III. RESULTS

The band structures of Bi_2Te_3, Bi_2Se_3, and Sb_2Te_3 have been studied extensively[7–11,13,15] due to their importance as room-temperature thermoelectric materials. The band structure of Sb_2Te_3 at ambient pressure is given in Fig. 2. Spin-orbit interactions, included here, play an important role in the band formation of Sb_2Te_3 (Ref. 13) as they do in Bi_2Te_3 (Refs. 7–10) and Bi_2Se_3 (Ref. 11) which has been described in detail in the cited publications.

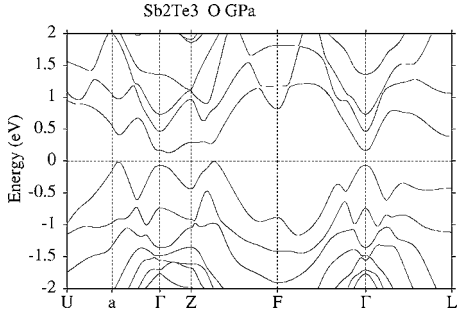

FIG. 2. Calculated band structure of Sb_2Te_3 at ambient pressure using the relaxed lattice constants.

When one looks at the band structure, plotted as it is for most compounds by calculating the eigenvalues along the high symmetry lines of the Brillouin zone, one finds two peaks close in energy, one along Γ-a and the other along Z-F. It is difficult to discern which of these forms the valence band maximum simply by sight. However, a recent calculation of Bi_2Te_3 by Youn and Freeman[10] showed that the position of the valence band maximum does not lie along these high symmetry lines but instead lies on the U-Γ-Z plane at a general point in k space. The valence band maximum lying on this plane has sixfold band degeneracy, consistent with Shubnikov–de Haas experiments.[2] Schiedemantel *et al.*[22] repeated these calculations in Bi_2Te_3 to find band extrema close, though not identical, to those found by Youn and Freeman.[10] While there exist many similarities between Bi_2Te_3 and Sb_2Te_3, these calculations were not repeated in the latter compound. Also, the positions of the band extrema have not been studied as a function of pressure in either compound.

A contour plot of the eigenvalues (Fig. 3) shows the positions of the high symmetry points (Γ, Z, F, L, U, and a) on the plane and the lines U-a-Γ and Z-F which are the symmetry lines which show the highest values in the valence band (Fig. 2). These lines show that, as in Bi_2Te_3,[10] the valence band maximum actually lies off the high symmetry lines plotted in Fig. 2. It is clear that the valence band maxima lies at a general point on this plane. The eigenvalues along Z-F lie closest to this maximum, though the values along Γ-a lie close in energy along a ridge extending from the upper left to near the middle of Fig. 3(a). This ridge of large eigenvalues in the box [Fig. 3(a)] has been reoriented and rescaled [Fig. 3(b)] to explore the details in this region. When this is done, the valence band maximum is seen to lie at the general position (0.693,0.595,0.595). The eigenvalues shown in Fig. 3(b) represent a doping level on the order of $10^{19}/cm^3$. The energy differences in the contour plot of the U-Γ-Z plane are 40 meV while they are only 14 meV for the values in the smaller region in order to better show the contrast.

As mentioned earlier,[9,10,12–15,20] the position and number of band extrema change the nature of the transport which is important for the thermoelectric properties. First, we look at the effects of hydrostatic pressure. Even though the pressure is hydrostatic, Sb_2Te_3 is a highly layered material where the c axis relaxes much faster than the a axis (Table I). The band structure has been calculated for 2.0 and 4.0 GPa, but the plot is nearly identical to that shown by Thonhauser *et al.*[13] so one is referred to this publication. As can been pointed out before, the bands lying away from E_F change, but the positions of the conduction and valence bands closest to E_F remain mostly unchanged.

In order to understand the position of the valence band maximum, contour plots are made for 2 and 4 GPa hydrostatic pressure (Fig. 4). Since the bands corresponding to the band extrema remained mostly unchanged in the plot along the high symmetry lines,[13] it is not surprising that the posi-

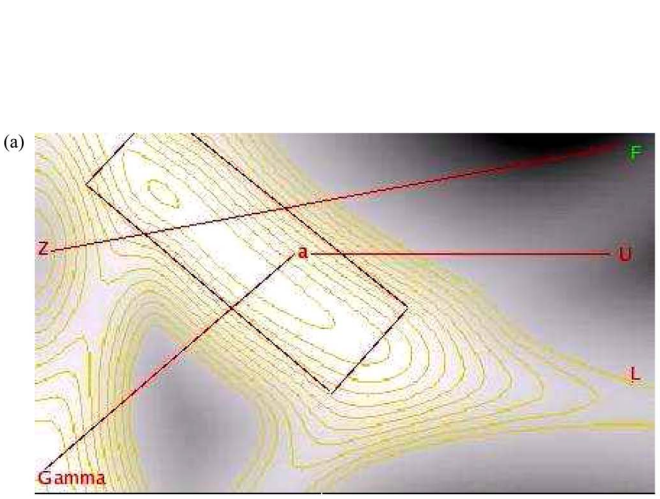

FIG. 3. (Color online) (a) Contour plot of the eigenvalues lying along the U-Γ-Z plane. Γ-Z lies in the perpendicular direction while Z-U lies horizontal near the middle of the plane. The valence band maximum does not lie along either high symmetry line. (b) The same contour plot associated with the values in the rectangle in (a). The plot has been rotated to align with the ridge of eigenvalues. Values increase from black at the lowest to white at the highest. The energy differences are 40 meV for (a) but only 14 meV for the plots corresponding to the smaller region (b).

tion of the valence band maximum remains mostly unchanged, lying close to where it lies under ambient pressure. As mentioned earlier, under hydrostatic pressure the thermoelectric properties are mostly flat up to 2 GPa and then decrease,[3] most likely due to an increase in the lattice thermal conductivity as the more rigid structure scatters fewer phonons. The position of the maximum changes slightly from (0.687,0.593,0.593) to (0.688,0.596,0.596) for 2 to 4 GPa, respectively, but this difference is not visible on the plots (Fig. 4). As before, the eigenvalues represent hole doping on the order of $10^{19}/\mathrm{cm}^3$.

The band structure shows a much more profound change under uniaxial pressure, even for smaller absolute values than in the hydrostatic case. In order to model the change in the lattice constant, one only needs to note that the lattice constants in Table I are linear as a function of pressure, so one can easily interpolate between the given values for 0.5 and 1.5 GPa. The values of u and v associated with the Sb and Te positions change little in Table I. Different values of u and v were tried close to the values in the table, but this made almost no change in the results. Uniaxial pressure causes the van der Waals layers to come closer together, leading to stronger interactions between the layers. The band gap arises from Sb and Te_1 atoms lying on the van der Waals gap,[8,9] so one expects to see changes in the position of the band extrema in this case. While one sees the peak along Z-F become lower than that along Γ-a (Fig. 5), this does not tell what happens to the position of the valence band maximum. At ambient pressure there appeared to be two peaks, one along Z-F and another along Γ-a, but this corresponded to one valence band maximum at (0.693,0.595,0.595).

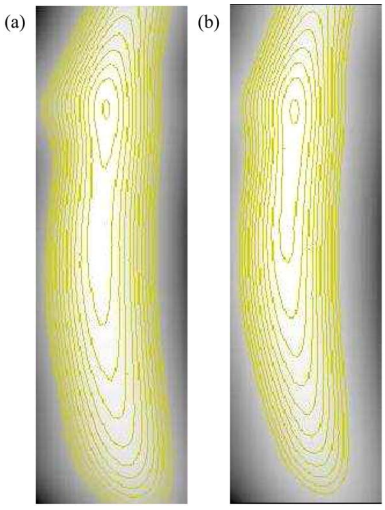

FIG. 4. (Color online) Contour plot of the eigenvalues lying along the ridge in the U-Γ-Z plane as in Fig. 3(b) for hydrostatic pressure of (a) 2 GPa and (b) 4 GPa. The eigenvalues represent hole doping on the order of $10^{19}/\mathrm{cm}^3$. The energy difference between the contour lines is 14 meV.

Looking carefully at the position of the valence band maximum on the contour plot shows significant changes even with relatively small uniaxial pressures (Fig. 6). The position of the valence band maximum changes slightly to (0.693,0.600,0.600) at 0.5 GPa, but a large range of similar maxima occur along the ridge extending to approximately (0.5,0.2,0.2). At 1.0 GPa the peak at (0.693,0.600,0.600) has 14 meV higher energy than the broad peak around (0.496,0.263,0.263). At 1.5 GPa the peak at (0.690,0.598,0.598) is 3.18 meV smaller than the new maximum at (0.477,0.222,0.222). At 2.0 GPa the maxima at (0.468,0.201,0.201) lies higher than the original peak at (0.690,0.600,0.600) by 27 meV. As a function of uniaxial pressure, the position of the valence band maximum shifts in the Brillouin zone. Most important is the effect near 1.5 GPa where there are multiple valence band maxima at nearly the

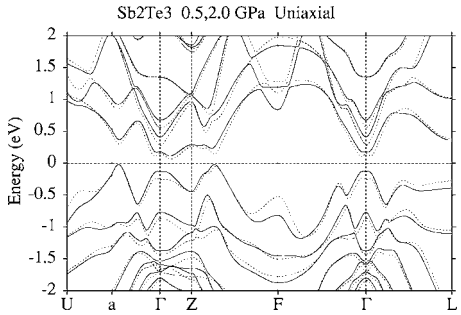

FIG. 5. Band structures of Sb_2Te_3 for uniaxial pressure of 0.5 (solid lines) and 2.0 GPa (dashed lines).

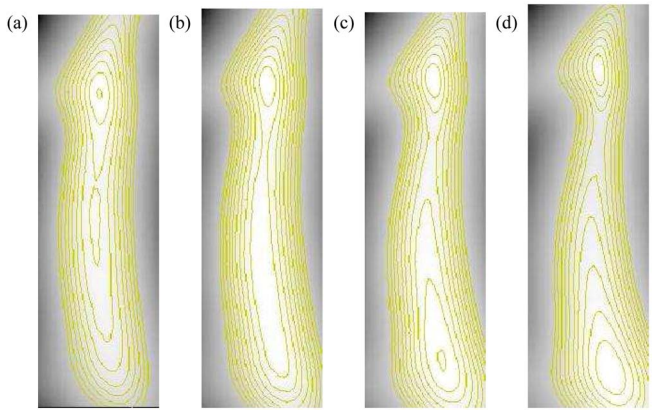

FIG. 6. (Color online) Contour plot of the eigenvalues lying along the ridge in the U-Γ-Z plane as in Fig. 3(b) for uniaxial pressure of (a) 0.5 GPa, (b) 1.0 GPa, (c) 1.5 GPa, and (d) 2.0 GPa. The eigenvalues represent hole doping on the order of $10^{19}/\mathrm{cm}^3$. The energy difference between the contour lines is 14 meV.

same energy which can all contribute to the conduction, thereby increasing the degeneracy factor γ in the B parameter[18,19] which leads to a larger carrier concentration without decreasing S and, hence, a larger value of ZT.[9]

As explained earlier, the parameter B, which increases along with ZT, is proportional to the degeneracy factor γ.[10,12,18–20] When the valence band maximum at (0.477,0.222,0.222) has approximately the same value as the original peak at (0.693,0.600,0.600) for 1.5 GPa, both of these valence band pockets can be filled with holes which increase γ from 6 to 12. This may be the electronic explanation for the increase in ZT ~2 GPa in $Sb_{1.5}Bi_{0.5}Te_3$.[6] As had been suggested by Polvani *et al.*[6] an electronic topological transition[28] (ETT) occurs in Sb_2Te_3 between 1 and 2 GPa applied uniaxially. The change from one sixfold peak to an additional sixfold peak having the same energy significantly changes the shape of the Fermi surface.[17,29] Such an ETT has been observed for Bi_2Te_3 with a sharp increase in ZT for hydrostatic pressure around 2 GPa,[17] though this transition has not yet been studied theoretically. The return to a single sixfold degenerate band at (0.468,0.201,0.201) explains the downturn in ZT after going through this transition above ~3 GPa. The band gap also reduces under uniaxial pressure, with the onset of metallicity at ~2.5 GPa (Ref. 13 and 17) which also causes ZT to decrease. Upon going from high pressure down to low pressure the peak shifts closer to 1 GPa, so the exact position of the onset of multiple valence band maxima may not be clear experimentally. Further calculations should be done on $Sb_{1.5}Bi_{0.5}Te_3$ as well as experiments on Sb_2Te_3 itself under uniaxial pressure to determine whether this explanation holds for both compounds and how the transition pressure changes with Bi doping.

As mentioned earlier, Shubnikov–de Haas measurements provide a model of the valence band of Sb_2Te_3 consisting of an upper valence band (UVB) with lighter holes and a lower valence band (LVB) with heavier holes.[2] The separation between these two bands is strongly dependent on the the doping. While the effective masses in Bi_2Te_3 are well known[30] and have been compared to electronic structure calculations,[9,14] those in Sb_2Te_3 are not as well understood.[2] The effective masses of the valence band maxima under pressure are given in Table II. These values were fit for occupations about $10^{18}/\mathrm{cm}^3$, close to the peak region. The fixed band parameters which were taken from anisotropy of the Fermi surface[2] do not agree well for m_x but are better for m_y and m_z. It should also be noted that these values are extrapolated and not directly measured. The measured ratios of the effective masses are around 3 for both the UVB and LVB, consistent with m_x/m_y for both maxima in the table. One should note an important differences between the calculation and experiment. The electronic structure shown here does not have UVB and LVB as part of the valence bands at ambient pressure but has only one valence band maximum. The second valence band peak arises only under uniaxial pressure of ~1 GPa. It is unclear whether the second valence band at (0.477,0.222,0.222) corresponds to the LVB seen experimentally.[2] However, the new valence band peak which produces the ETT having a heavier effective mass explains the increase in the thermoelectric properties since the masses increases the B parameter,[12,18,19] not just the degeneracy factor γ.[10,20]

TABLE II. The effective masses of the valence band(s) in Sb_2Te_3 under both hydrostatic and uniaxial pressure. Also added are experimental fixed band parameters (Ref 2).

(GPa)	Position	m_x/m_e	m_y/m_e	m_z/m_e
0.0	(0.693,0.595,0.595)	0.17	0.06	0.13
0.0	Experiment (Ref. 2)	0.44	0.03	0.08
Hydrostatic				
2.0	(0.687,0.593,0.593)	0.17	0.06	0.18
4.0	(0.688,0.596,0.596)	0.15	0.04	0.16
Uniaxial				
0.5	(0.693,0.600,0.600)	0.18	0.07	0.21
1.0	(0.693,0.600,0.600)	0.20	0.07	0.20
1.5	(0.690,0.598,0.598)	0.18	0.06	0.17
1.5	(0.477,0.222,0.222)	0.29	0.12	0.22
2.0	(0.690,0.600,0.600)	0.19	0.07	0.17
2.0	(0.468,0.201,0.201)	0.34	0.14	0.21

One can see that there are significant differences between the position of the valence maxima in Bi_2Te_3 and Sb_2Te_3. Youn and Freeman[10] found the valence band maximum to lie at (0.546,0.383,0.383) which was higher by 3.8 meV than the peak at (0.665,0.586,0.586) even at ambient pressure. On the other hand, there exists only one peak in Sb_2Te_3 at ambient pressure at (0.693,0.595,0.595) with the second peak at (0.477,0.222,0.222) arising only under uniaxial pressure of ~1.5 GPa. Therefore, the ETT observed in Bi_2Te_3 (Ref. 17) must differ in how the bands rearrange under hydrostatic pressure.

IV. SUMMARY

Hydrostatic and uniaxial pressure can be tuned to change the band structure in order to enhance the thermoelectric

properties of Sb_2Te_3. Hydrostatic pressure shows little change in the position of the valence band maximum and little difference to the band structure as a whole aside from shifting bands which lie away from E_F. Uniaxial pressure shows a profound change in the band structure, especially the valence band maximum. The valence band maximum in Sb_2Te_3 lies off the high symmetry lines at (0.690,0.598,0.598) but shifts to (0.468,0.201,0.201) around 2.0 GPa uniaxial pressure. Around 1.5 GPa both peaks have approximately the same height, leading to two sets of sixfold degenerate bands which should enhance the band degeneracy and increase the value of *ZT*. This may be the electronic topological transition[6] which had been predicted for $Sb_{1.5}Bi_{0.5}Te_3$ as it shows a large increase in *ZT* under uniaxial pressure between 1 and 2 GPa. Not only is there an increase in the number of band extrema, γ, but the effective masses also get larger which further increases the *B* parameter and *ZT*.[10,12,18–20]

ACKNOWLEDGMENT

The author wishes to thank J. Dyck for many helpful discussions.

[1] A. A. Averkin, O. S. Gryaznov, and Yu. Z. Sanfirov, Fiz. Tekh. Poluprovodn. (S.-Petersburg) **12**, 2280 (1978).
[2] V. A. Kul'bachinskii, N. E. Klokova, Ya. Gorak, P. Loshytak, S. A. Azou, and G. A. Mironova, Fiz. Tverd. Tela (Leningrad) **31**, 205 (1989); V. A. Kul'bachinskii, N. B. Brandt, P. A. Cherenmykh, S. A. Azou, J. Horak, and and P. Lostak, Phys. Status Solidi B **150**, 237 (1988).
[3] L. G. Khvostantsev, A. I. Orlov, N. Kh. Abrikosov, and L. D. Ivanova, Phys. Status Solidi A **58**, 37 (1980); L. G. Khvostantsev, A. I. Orlov, N. Kh. Abrikosov, and L. D. Ivanova, *ibid.* **89**, 301 (1985).
[4] N. Sakai, T. Kajiwara, K. Takemura, S. Minomura, and Y. Fujii, Solid State Commun. **40**, 1045 (1981).
[5] B. Rönnlund, O. Beckman, and H. Levy, J. Phys. Chem. Solids **26**, 1281 (1965).
[6] D. A. Polvani, J. F. Meng, N. V. Cahndra Shekar, J. Sharp, and J. V. Badding, Chem. Mater. **13**, 2068 (2001).
[7] G. A. Thomas, D. H. Rapke, R. B. Van Dover, L. F. Mattheis, W. A. Surden, L. F. Schneemaper, and J. V. Waszczak, Phys. Rev. B **46**, 1553 (1992).
[8] S. K. Mishra, S. Satpathy, and O. Jepsen, J. Phys.: Condens. Matter **91**, 461 (1997).
[9] P. Larson, S. D. Mahanti, and M. G. Kanatzidis, Phys. Rev. B **61**, 8162 (2000).
[10] S. J. Youn and A. J. Freeman, Phys. Rev. B **63**, 085112 (2001).
[11] P. Larson, Phys. Rev. B **68**, 155121 (2003).
[12] G. Chen, M. S. Dresselhaus, G. Dresselhaus, J.-P. Fleurial, and T. Caillat, Int. Mater. Rev. **48**, 45 (2003).
[13] T. Thonhauser, T. J. Scheidemantel, J. O. Sofo, J. V. Badding, and G. D. Mahan, Phys. Rev. B **68**, 085201 (2003).
[14] M. Kim, A. J. Freeman, and C. B. Geller, Phys. Rev. B **72**, 035205 (2005).
[15] T. Thonhauser, G. S. Jeon, G. D. Mahan, and J. O. Sofo, Phys. Rev. B **68**, 205207 (2003).
[16] G. Mahan, B. Sales, and J. Sharp, Phys. Today **50**, 42 (1997).
[17] E. S. Itsekevich, L. M. Kashirskaya, and V. F. Kraidenov, Semiconductors **31**, 276 (1996).
[18] G. D. Mahan, J. Appl. Phys. **65**, 1578 (1989).
[19] L. D. Hicks and M. S. Dresselhaus, Phys. Rev. B **47**, 12727 (1993).
[20] G. Yonghui and X. Jingying, Chem. J. Internet **7**, 072019re (2005).
[21] R. Chasmar and R. Stratton, J. Electron. Control **7**, 52 (1959).
[22] T. J. Schiedemantel, C. Ambrosch-Draxl, T. Thonhauser, J. V. Badding, and J. O. Sofo, Phys. Rev. B **68**, 125210 (2003).
[23] C.-Y. Li, A. L. Ruoff, and C. W. Spencer, J. Appl. Phys. **32**, 1733 (1961).
[24] R. W. G. Wyckoff, *Crystal Structures* (Krieger, Melbourne, FL, 1986), Vol. 2.
[25] P. Hohenberg and W. Kohn, Phys. Rev. **136**, B864 (1964); W. Kohn and L. J. Sham, *ibid.* **140**, A1133 (1965).
[26] M. Methfessel, M. van Schilfgaarde, and R. A. Casali, in *Electronic Structure and Physical Properties of Solids, The Uses of the LMTO Method*, edited by Hughes Dreysse, Springer Lecture Notes, Workshop Mont Saint Odille, France, 1998 (Springer, Berlin, 2000), p. 114–147.
[27] U. von Barth and L. Hedin, J. Phys. C **5**, 2064 (1972).
[28] I. M. Lifshitz, Sov. Phys. JETP **11**, 1130 (1960).
[29] Y. M. Blanter, M. I. Kaganov, A. V. Pantsulaya, and A. A. Varlamov, Phys. Rep. **245**, 159 (1994).
[30] H. Kohler, Phys. Status Solidi B **73**, 95 (1976); *ibid.* **74**, 591 (1976).